

# Energy density at kinetic freeze-out in Pb-Pb collisions at the LHC using the Tsallis distribution

M. D. Azmi<sup>1</sup>, T. Bhattacharyya<sup>2</sup>, J. Cleymans<sup>3</sup>  
and M. Paradza<sup>3</sup>

<sup>1</sup> Physics Department, Aligarh Muslim University, Aligarh-202002 (U.P.), India

<sup>2</sup> Bogoliubov Laboratory of Theoretical Physics, JINR, Dubna, 141980, Moscow region, Russia

<sup>3</sup>UCT-CERN Research Centre and Department of Physics, University of Cape Town, Rondebosch 7701, South Africa

**Abstract.** The thermodynamic parameters like energy density, pressure, entropy density, temperature and particle density are determined from the transverse momentum distributions of charged particles in Pb-Pb collisions at the LHC. The results show a clear increase with the centrality and the beam energy in all parameters. It is determined that in the final freeze-out stage the energy density reaches a value of about 0.039 GeV/fm<sup>3</sup> for the most central collisions at  $\sqrt{s_{NN}} = 5.02$  TeV. This is less than that at chemical freeze-out where the energy density is about 0.36 GeV/fm<sup>3</sup>. This decrease approximately follows a  $T^4$  law. The results for the pressure and entropy density are also presented for each centrality class at  $\sqrt{s_{NN}} = 2.76$  and 5.02 TeV.

PACS numbers: 12.40.Ee, 25.75.Dw, 13.85.Ni, 24.10.Pa

## 1. Introduction

In heavy-ion collisions at the Large Hadron Collider (LHC) hadronic matter is created at a very high energy density. After the initial very hot stage, the system expands, reaches chemical equilibrium and then finally freezes-out in a stage usually referred to as the kinetic freeze-out stage. The present paper determines the energy density, the pressure, the entropy density and the particle density at this final kinetic freeze-out stage using the transverse momentum distributions of charged particles measured by the ALICE collaboration in Pb-Pb collisions at  $\sqrt{s_{NN}} = 2.76$  and 5.02 TeV [1]. For this purpose one needs a description which is thermodynamically consistent, i.e. the following relations must be satisfied:

$$d\epsilon = T ds + \mu dn, \quad (1)$$

$$dP = s dT + n d\mu, \quad (2)$$

where  $\epsilon$  is the energy density,  $T$  is the temperature,  $s$  is the entropy density,  $P$  is the pressure,  $\mu$  is the chemical potential and  $n$  is the particle density. The Maxwell relations

given below follow from this:

$$T = \left. \frac{\partial \epsilon}{\partial s} \right|_n, \quad \mu = \left. \frac{\partial \epsilon}{\partial n} \right|_s, \quad (3)$$

$$n = \left. \frac{\partial P}{\partial \mu} \right|_T, \quad s = \left. \frac{\partial P}{\partial T} \right|_\mu. \quad (4)$$

The following thermodynamic relation must also be satisfied:

$$\epsilon + P = Ts + \mu n. \quad (5)$$

Such a description does exist. It is based on the Tsallis distribution [2] given by:

$$f(E, q, T, \mu) \equiv \left( 1 + (q-1) \frac{E - \mu}{T} \right)^{-\frac{1}{q-1}}, \quad (6)$$

where  $E$  is the energy of the particle,  $q$  is the Tsallis parameter which, when approaching 1, makes the function  $f$  exponential (Boltzmann-like). The chemical potential  $\mu$  will be taken to be zero in the present analysis presented below as is appropriate in the central rapidity region at LHC energies. The parameter  $q$  has been related to the relative variance of a superposition of Boltzmann-Gibbs distributions [3]. The function in equation (6) can be expressed as a superposition of Boltzmann like functions with different temperature values [3].

There exist other, closely related, distributions that have been used to describe transverse momentum spectra, see [4, 5, 6, 7, 8, 9] but these do not offer the advantage of connecting to a full thermodynamic description for the relevant thermodynamic variables discussed here.

The relevant thermodynamic quantities can be obtained from the following relations

$$s = -g \int \frac{d^3p}{(2\pi)^3} (f^q \ln_q f - f), \quad (7)$$

$$n = g \int \frac{d^3p}{(2\pi)^3} f^q, \quad (8)$$

$$\epsilon = g \int \frac{d^3p}{(2\pi)^3} E f^q, \quad (9)$$

$$P = g \int \frac{d^3p}{(2\pi)^3} \frac{p^2}{3E} f^q, \quad (10)$$

where  $g$  is the usual degeneracy factor and

$$\ln_q f \equiv \frac{f^{1-q} - 1}{1 - q}. \quad (11)$$

The derivation has been presented in detail in [10, 11]. It has also been shown that it leads to a surprisingly good fit of transverse momentum distributions up to  $p_T$  values of 200 GeV/c [12, 13, 14, 15]. A comprehensive comparison with experimental results has been presented in [16] for pp collisions.

Our paper is organized as follows. In section 2 we discuss the single particle distribution which we use for fitting the transverse momentum spectra of the charged

hadrons, and determine the temperature  $T$  and the Tsallis parameter  $q$ . In section 3 we calculate the corresponding thermodynamic quantities namely, the energy density, the pressure, the entropy density and the particle density. The values obtained for the energy density are then discussed and compared to values obtained at different stages of the collision and to other closely related energy densities. Lastly, we summarize our results and conclude in section 4.

## 2. Transverse Momentum Distribution

The Tsallis distribution was first proposed more than three decades ago as a generalization of the Boltzmann-Gibbs distribution [2], and is characterized by only three parameters namely, the Tsallis parameter  $q$ , the temperature  $T$  and the volume  $V$ .

The momentum distribution of particles obtained by using the expression for the particle density given in equation (8) is written as:

$$\frac{d^3N}{d^3p} = \frac{gV}{(2\pi)^3} \left[ 1 + (q-1) \frac{E - \mu}{T} \right]^{-q/(q-1)}. \quad (12)$$

When expressed in terms of transverse momentum,  $p_T$ , transverse mass,  $m_T = \sqrt{p_T^2 + m^2}$  and rapidity,  $y$ , the above equation takes the following form:

$$\frac{d^2N}{dp_T dy} = gV \frac{p_T m_T \cosh y}{(2\pi)^2} \left[ 1 + (q-1) \frac{m_T \cosh y - \mu}{T} \right]^{-q/(q-1)}. \quad (13)$$

At mid-rapidity,  $y = 0$ , and for zero chemical potential, as is relevant at the LHC, equation (13) reduces to the following expression:

$$\left. \frac{d^2N}{dp_T dy} \right|_{y=0} = gV \frac{p_T m_T}{(2\pi)^2} \left[ 1 + (q-1) \frac{m_T}{T} \right]^{-q/(q-1)}. \quad (14)$$

The transverse momentum distributions of charged particles produced in Pb-Pb collisions at LHC energies are fitted using a sum of three Tsallis distributions. These consist of fits for  $\pi^+$ 's,  $K^+$ 's and protons. The following expression, at mid-rapidity and  $\mu = 0$ , was used to fit the pseudo-rapidity distributions:

$$\frac{d^2N_{ch}}{dp_T d\eta} = 2p_T \frac{V}{(2\pi)^2} \sum_{i=1}^3 g_i m_{T,i} \frac{p_T}{m_{T,i}} \left[ 1 + (q-1) \frac{m_{T,i}}{T} \right]^{-\frac{q}{(q-1)}} \quad (15)$$

where  $i = \pi^+, K^+, p$ . The relative weights between particles are given by the corresponding degeneracy factors  $g_{\pi^+} = g_{K^+} = 1$  and  $g_p = 2$ . The factor 2 on the right hand side takes into account the contributions from antiparticles,  $\pi^-, K^-$  and  $\bar{p}$ . The extra factor  $p_T/m_T$  on the right hand side takes into account the change from rapidity to pseudo-rapidity using the relation:

$$\frac{dN}{dp_T d\eta} = \sqrt{1 - \frac{m^2}{m_T^2 \cosh^2 y}} \frac{dN}{dy dp_T}, \quad (16)$$

which, at mid-rapidity, becomes:

$$\frac{dN}{dp_T d\eta} = \frac{p_T}{m_T} \frac{dN}{dp_T dy}, \quad (17)$$

hence the extra factor of  $p_T/m_T$ .

The resulting fits to the experimental data obtained in Pb-Pb collisions at  $\sqrt{s_{NN}} = 2.76$  TeV [1] are shown in figure 1 where we follow the centrality classification introduced in [1]. As can be seen in figure 1 the fits are very good for peripheral events and at low, gradually worsening for the more central events where the fits at first overshoot the data above  $p_T$  values of about 3 GeV then rejoin the data and at larger values of  $p_T$  above about 20 GeV are below the data. The same behaviour can be seen for a beam energy of 5.02 TeV in figure 2. We have checked that the same behaviour is also present in Xe-Xe collisions [17] at 5.44 TeV. The transverse momentum distributions tend to show an S shape for central collisions, this shape is difficult to reproduce using the Tsallis parameterization which has only two variables  $T$  and  $q$  and the overall normalization fixed by the volume  $V$ . Clearly one more parameter would be needed to reproduce the shape for the most central events.

In table 1 we collect all the results for the temperature  $T$  and the Tsallis parameter  $q$  obtained from fitting the Pb-Pb data at a beam energy of 2.76 TeV. Note that the temperature varies from just slightly above 96 MeV for the most central events and to about 78 MeV for the most peripheral events. The results obtained this way are consistent with those obtained in analyses using the blast-wave [18] formalism [19, 20] but they are considerably lower than those obtained recently in [21, 22]. As usual, the Tsallis parameter  $q$  can be determined with an excellent accuracy.

**Table 1.** Values of  $q$ ,  $T$  and  $\chi^2/\text{NDF}$  obtained using equation (14) to fit the data at  $\sqrt{s_{NN}} = 2.76$  TeV [1].

Centrality	Class	$q$	$T$ (MeV)	$\chi^2/\text{NDF}$
1	(0-5)%	$1.1355 \pm 8.74\text{e-}04$	$95.87 \pm 1.36$	156.5/58
2	(5-10)%	$1.1363 \pm 8.86\text{e-}04$	$95.54 \pm 1.32$	150.4/58
3	(10-20)%	$1.1375 \pm 8.61\text{e-}04$	$94.56 \pm 1.29$	138.6/58
4	(20-30)%	$1.1387 \pm 8.81\text{e-}04$	$92.87 \pm 1.30$	117.3/58
5	(30-40)%	$1.1389 \pm 9.08\text{e-}04$	$91.22 \pm 1.29$	91.5/58
6	(40-50)%	$1.1403 \pm 9.34\text{e-}04$	$88.04 \pm 1.27$	71.4/58
7	(50-60)%	$1.1416 \pm 9.75\text{e-}04$	$84.56 \pm 1.25$	52.8/58
8	(60-70)%	$1.1424 \pm 1.04\text{e-}03$	$81.05 \pm 1.27$	36.35/58
9	(70-80)%	$1.1428 \pm 1.16\text{e-}03$	$78.01 \pm 1.31$	26.4/58

The fits to the experimental data at 5.02 TeV are shown in figure 2 where, as before, we follow the centrality classification from [1]. Again the fits are very good for peripheral events, gradually worsening for the more central events where the fits at first overshoot the data above  $p_T$  values of 2 GeV; then gradually rejoin the data at larger values of  $p_T$  and in the end overshoot the data.

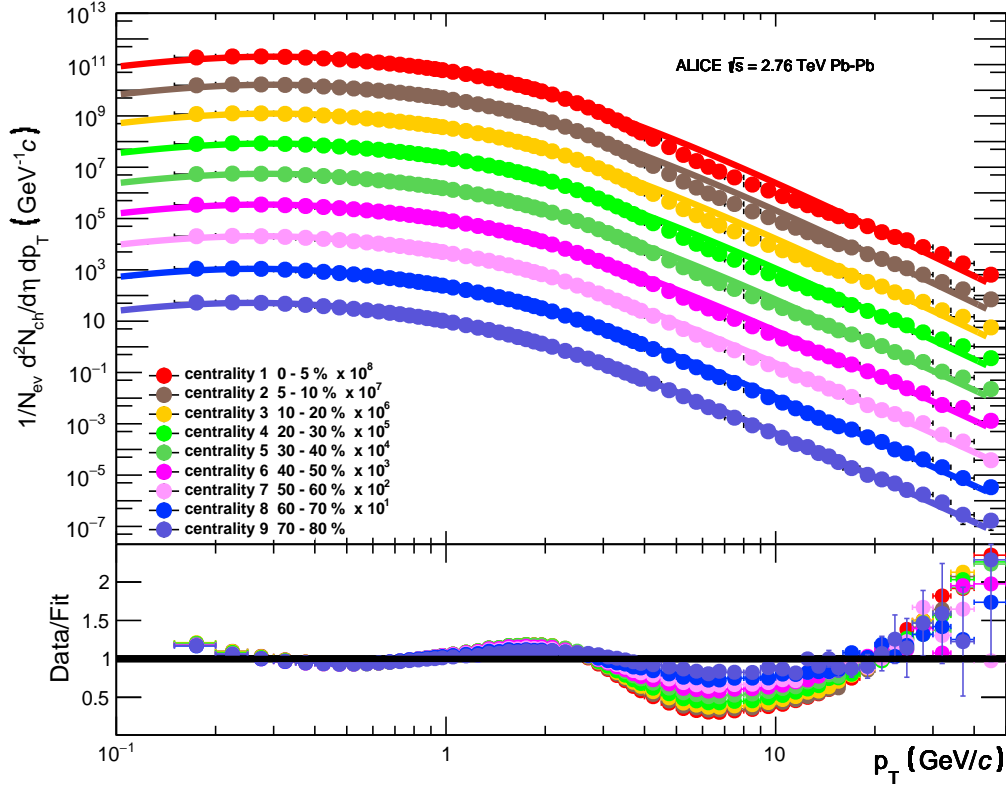


**Figure 1.** Transverse momentum distributions measured by the ALICE collaboration in Pb-Pb collisions at  $\sqrt{s_{NN}} = 2.76$  TeV [1] for different centrality classes. The solid lines represent fits made using the Tsallis distribution equation (15). The lower part of the figure shows the ratio of the data divided by the fit value.

Similar to the procedure followed above, we collect in table 2 the results for the temperature  $T$  and the Tsallis parameter  $q$  obtained from fitting the Pb-Pb data at  $\sqrt{s_{NN}} = 5.02$  TeV. As in the previous case one has a very good description of the transverse momentum distributions for the most peripheral collisions, again gradually worsening for the most central events where the fits at first overshoot the data at large values of  $p_T$  and in the end are below the data. The temperature  $T$  and the Tsallis parameter  $q$  have been determined at the two beam energies for all the centrality classes. Using the values obtained

### 3. Thermodynamic Variables

#### 3.1. Energy Density at Kinetic Freeze-Out

Having deduced the temperature  $T$  and the Tsallis parameter  $q$  at kinetic freeze-out from the transverse momentum distributions for two beam energies, we now proceed

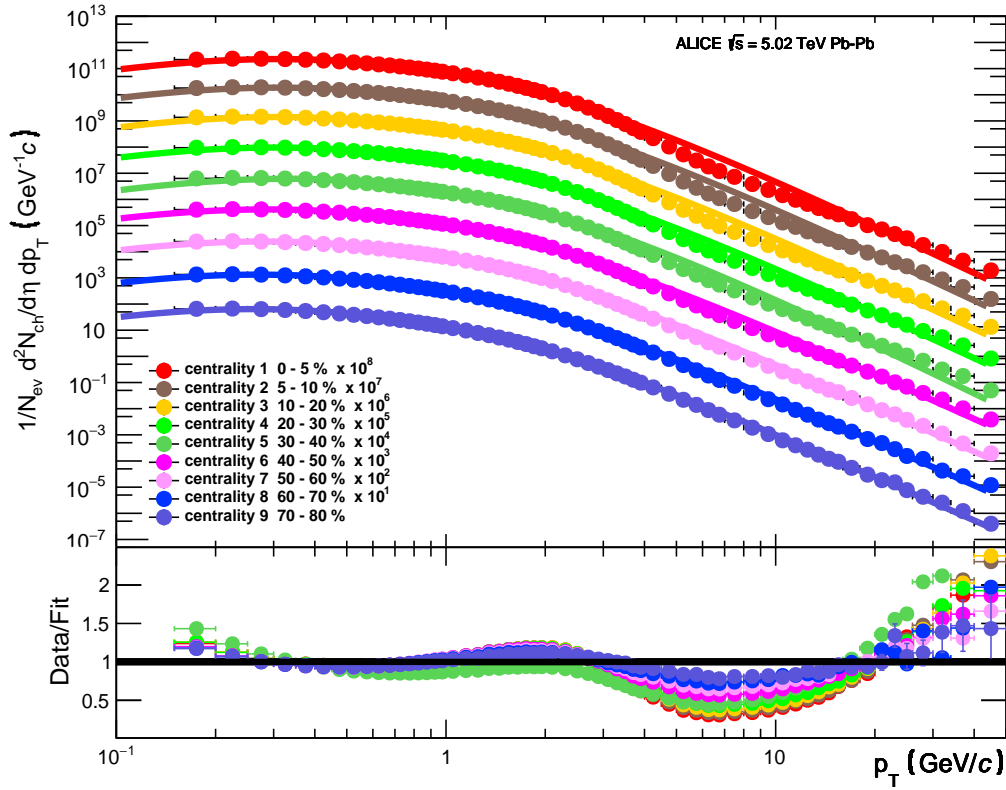


**Figure 2.** Transverse momentum distributions measured by the ALICE collaboration in Pb-Pb collisions at  $\sqrt{s_{NN}} = 5.02$  TeV [1] for different centrality classes. The solid lines are fits using the Tsallis distribution (15). The lower part of the figure shows the ratio of the data divided by the fit value.

**Table 2.** Values of  $q$ ,  $T$  and  $\chi^2/\text{NDF}$  obtained using equation (14) to fit the data at  $\sqrt{s_{NN}} = 5.02$  TeV [1].

Centrality Class	$q$	$T$ (MeV)	$\chi^2/\text{NDF}$
1 (0-5)%	$1.1405 \pm 8.65\text{e-}04$	$98.18 \pm 1.33$	163.8/58
2 (5-10)%	$1.1413 \pm 8.81\text{e-}04$	$97.78 \pm 1.36$	154.4/58
3 (10-20)%	$1.1423 \pm 8.76\text{e-}04$	$96.80 \pm 1.29$	142.7/58
4 (20-30)%	$1.1438 \pm 8.74\text{e-}04$	$94.84 \pm 1.23$	126.6/58
5 (30-40)%	$1.1449 \pm 8.97\text{e-}04$	$92.53 \pm 1.23$	104.9/58
6 (40-50)%	$1.1467 \pm 8.96\text{e-}04$	$89.80 \pm 1.21$	86.2/58
7 (50-60)%	$1.1477 \pm 9.18\text{e-}04$	$85.32 \pm 1.17$	61.6/58
8 (60-70)%	$1.1489 \pm 9.44\text{e-}04$	$81.30 \pm 1.13$	45.4/58
9 (70-80)%	$1.1504 \pm 1.01\text{e-}03$	$77.44 \pm 1.16$	35.4/58

calculating the energy density given by equation (9):

$$\epsilon = 2 \sum_{i=1}^3 g_i \int \frac{d^3p}{(2\pi)^3} E_i \left( 1 + (q-1) \frac{E_i}{T} \right)^{-\frac{q}{q-1}}, \quad (18)$$

**Table 3.** Values for the energy density, expressed in  $\text{GeV}/\text{fm}^3$ , obtained using equation (9) for the different centrality classes. The energy density at chemical freeze-out has been calculated at  $T = 156 \text{ MeV}$ .

Centrality Class	$\epsilon$ at 2.76 TeV	$\epsilon$ at 5.02 TeV
1 (0-5)%	0.0327164	0.0393321
2 (5-10)%	0.0321844	0.0385986
3 (10-20)%	0.0315327	0.0373159
4 (20-30)%	0.029377	0.0348676
5 (30-40)%	0.0269626	0.031484
6 (40-50)%	0.0233944	0.0266861
7 (50-60)%	0.0196353	0.0224109
8 (60-70)%	0.0160376	0.0180916
9 (70-80)%	0.0135606	0.0145837
proton [23]	0.334	
chemical freeze-out [24]	0.359	
lattice QCD [25]	$0.34 \pm 0.16$	
cold nuclear matter	0.16	

where  $i = \pi^+, K^+, p$ . The relative weights between particles are given by the corresponding degeneracy factors  $g_{\pi^+} = g_{K^+} = 1$  and  $g_p = 2$ . The factor 2 on the right hand side takes into account the contributions from antiparticles,  $\pi^-$ ,  $K^-$  and  $\bar{p}$ . The results are shown in figure 3 as a function of centrality. It is not unexpected that the values are slightly higher at a beam energy of 5.02 TeV than at 2.76 TeV.

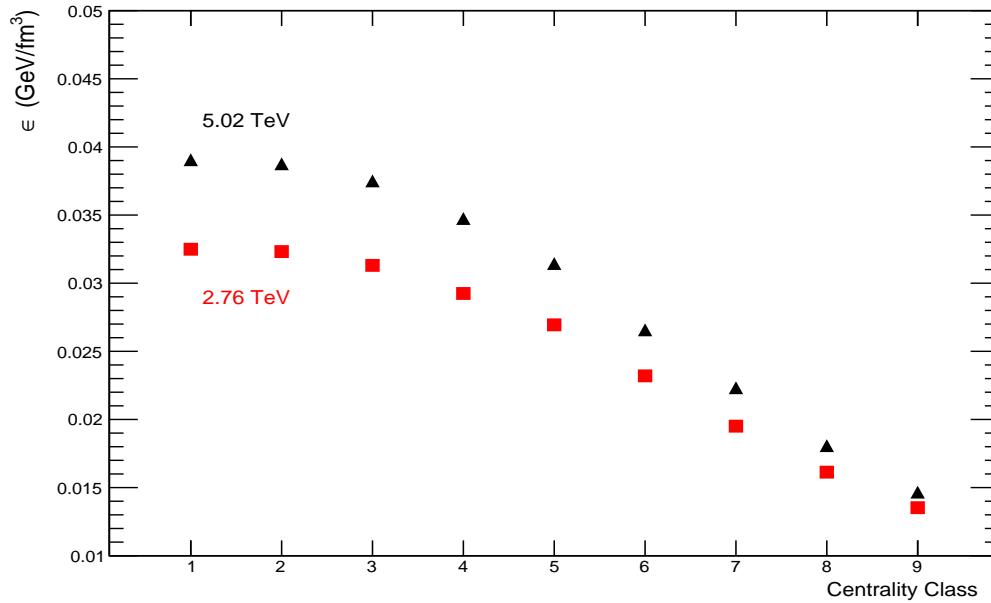


**Figure 3.** Energy density at kinetic freeze-out in Pb-Pb collisions at 2.76 and 5.02 TeV [1] as a function of centrality class calculated using equation (9).

In table 3 we collect all the results obtained for the energy density thus far and compare with a few other energy densities. The entry for the chemical freeze-out energy density has been obtained using the latest version of THERMUS [24] ‡. The latter has been calculated from all hadronic resonances and is not limited to the charged particles only. It has been shown recently that the chemical freeze-out temperature is approximately independent of centrality [26, 27]. For comparison we also show the energy density inside a proton calculated using the charge radius of the proton given as 0.875 fm and the mass of the proton as listed in the PDG [23]. The difference between the kinetic and chemical freeze-out results is not surprising in view of the fact that the energy density changes as  $T^4$  for massless particles. In table 3 we also show the energy density obtained in the phase transition region obtained using Lattice QCD [25].

### 3.2. Pressure at Kinetic Freeze-Out

The pressure plays an important role in the hydrodynamic description of heavy-ion collisions, e.g. in the study of shock waves or the speed of sound in a hadronic gas. In the present analysis, the pressure can be determined explicitly from the following equation (10):

$$P = 2 \sum_{i=1}^3 g_i \int \frac{d^3p}{(2\pi)^3} \frac{p^2}{3E_i} \left( 1 + (q-1) \frac{E_i}{T} \right)^{-\frac{q}{q-1}}, \quad (19)$$

where  $i = \pi^+, K^+, p$ . The relative weights between particles are given by the corresponding degeneracy factors  $g_{\pi^+} = g_{K^+} = 1$  and  $g_p = 2$ . As previously, the factor 2 on the right hand side takes into account the contributions from antiparticles,  $\pi^-, K^-$  and  $\bar{p}$ .

The results are shown in figure 4 where one notices a clear, expected, increase in the pressure when going from peripheral collisions to central ones. We have also checked explicitly that the inequality:

$$\epsilon \geq 3P, \quad (20)$$

is always satisfied.

### 3.3. Entropy Density at Kinetic Freeze-Out

The entropy is an important quantity because it plays a major role in hydrodynamic expansion calculations where entropy is sometimes assumed to be conserved when going from the quark-gluon plasma phase to the hadronic phase. This is for example the case in the Bjorken model [28] and other model calculations. It is difficult to relate it directly to a measurable quantity and it is often indirectly linked to the particle number. In this paper the connection is a fairly direct one and can be obtained using equation (7). More explicitly, the entropy density is given by the following expression where the parameters

‡ B. Hippolyte and Y. Schutz, <https://github.com/thermus-project/THERMUS>



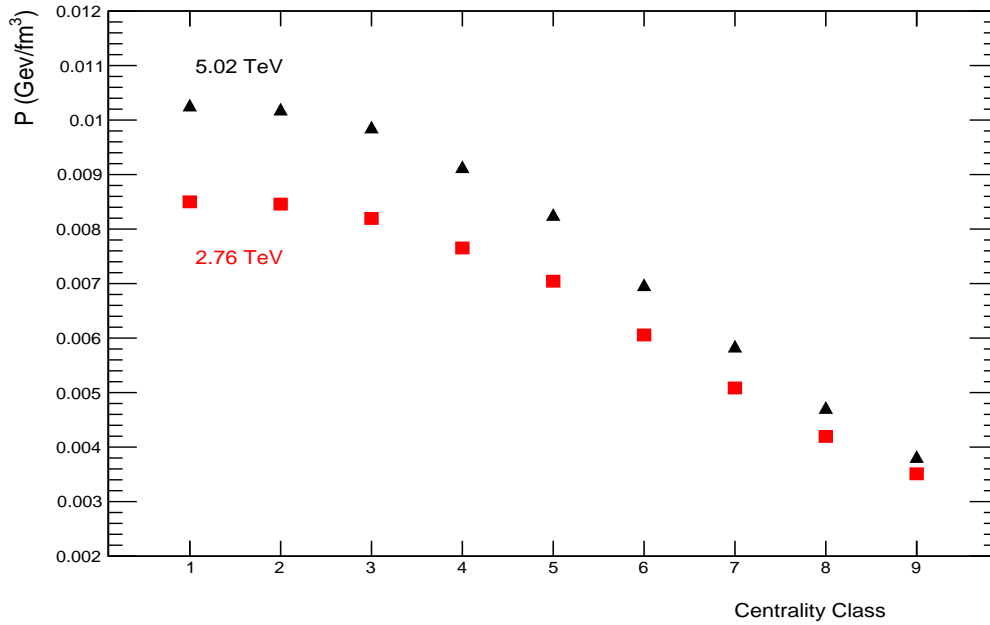


**Figure 4.** Pressure at kinetic freeze-out in Pb-Pb collisions at 2.76 and 5.02 TeV [1] as a function of centrality class calculated using equation (10).

$T$  and  $q$  are taken from table 1 for Pb-Pb collisions at  $\sqrt{s_{NN}} = 2.76$  TeV and table 2 for collisions at 5.02 TeV respectively:

$$s = 2 \sum_{i=1}^3 g_i \int \frac{d^3p}{(2\pi)^3} \left[ \frac{E_i}{T} \left( 1 + (q-1) \frac{E_i}{T} \right)^{-\frac{q}{q-1}} + \left( 1 + (q-1) \frac{E_i}{T} \right)^{-\frac{1}{q-1}} \right], \quad (21)$$

where, as before,  $i = \pi^+, K^+, p$ . The relative weights between particles are given, as before, by the corresponding degeneracy factors and given by  $g_{\pi^+} = g_{K^+} = 1$  and  $g_p = 2$ . The factor 2 on the right hand side, as previously, takes into account the contributions from antiparticles,  $\pi^-, K^-$  and  $\bar{p}$ . The results are shown in figure 5 where one can see a clear increase in the entropy density as we go from peripheral to central collisions. There is also a small increase when the beam energy is increased from  $\sqrt{s_{NN}} = 2.76$  to 5.02 TeV. We have also checked explicitly that the thermodynamic relation,

$$\epsilon + P = Ts, \quad (22)$$

holds. This is further confirmation of the consistency of having the chemical potential  $\mu$  equal to zero for the collisions under consideration. As this is done at kinetic freeze-out and not at chemical freeze-out, this is a non-trivial observation. At chemical freeze-out the chemical potentials must be zero because of the equal numbers of particles and antiparticles. At thermal freeze-out however it is only required that the chemical potentials for particles and antiparticles be equal but not necessarily zero.

For completeness we show the particle density calculated using equation (8) in figure 6. This is clearly well below the interior density of a heavy nucleus which is 0.17 nucleons/fm<sup>3</sup> [23].

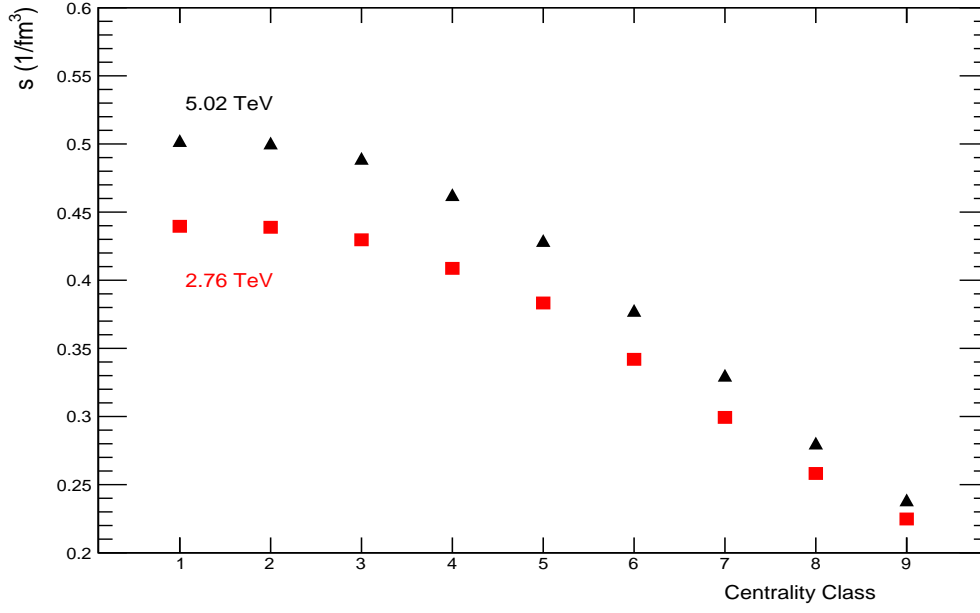


**Figure 5.** Entropy density at kinetic freeze-out in Pb-Pb collisions at 2.76 and 5.02 TeV [1] as a function of centrality class calculated using equation (7) .

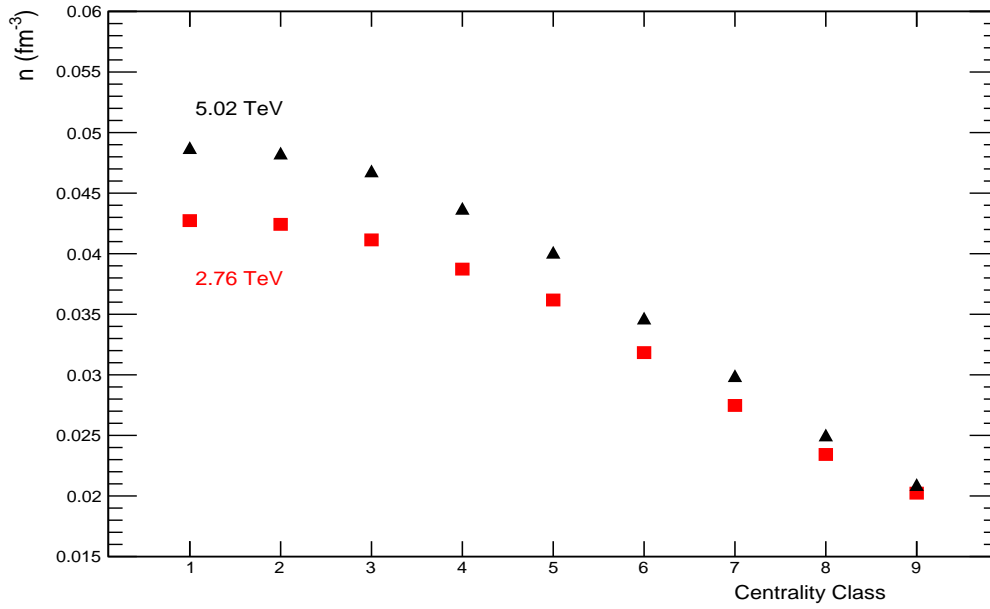


**Figure 6.** Particle density at kinetic freeze-out in Pb-Pb collisions at 2.76 and 5.02 TeV [1] as a function of centrality calculated using equation (8) .

#### 4. Summary

The transverse momentum distributions of the primary charged particles measured in Pb - Pb collisions at  $\sqrt{s_{NN}} = 2.76$  and 5.02 TeV by the ALICE collaboration [1] have been analysed in this paper using a thermodynamically consistent form of the Tsallis distribution based on equation (6). This gives a very good description of the transverse momentum distributions for the most peripheral collisions, gradually worsening for the most central events where the fits at first overshoot the data at large values of  $p_T$  and in the end are below the data, which is a matter of further exploration. The temperature  $T$  and the Tsallis parameter  $q$  have been determined at the two beam energies for all the centrality classes. Using the values obtained we then determined the energy density,  $\epsilon$ , pressure,  $P$ , entropy density,  $s$  and the particle density,  $n$  at kinetic freeze-out. as a function of the centrality classes. As expected, the values of all the thermodynamic quantities show an increase towards higher centrality class and at higher beam energy. It is determined that in the final freeze-out stage the energy density reaches a value of about 0.039 GeV/fm<sup>3</sup> for the most central collisions at  $\sqrt{s_{NN}} = 5.02$  TeV. This is less than that at chemical freeze-out where the energy density is about 0.36 GeV/fm<sup>3</sup>. This decrease approximately follows a  $T^4$  law. It can be concluded that, together with the results obtained at chemical freeze-out, the thermodynamic quantities presented in this paper provide information about the evolution of the thermodynamic quantities during the evolution of the hadronic phase from chemical to kinetic freeze-out.

#### Acknowledgments

One of us (T.B.) acknowledges partial support from the joint research projects between the JINR and IFIN-HH. We thank Smbat Grigoryan for helpful comments.

## References

- [1] Acharya S et al. 2018 *J. High Energy Phys.* **11** 013
- [2] Tsallis C 1988 *J. Statist. Phys.* **52** 479 1988
- [3] Wilk A and Wlodarczyk Z 2000 *Phys. Rev. Lett.* **84** 2770
- [4] Abelev B B et al. 2013 *Eur. Phys. J. C* **73** 2662
- [5] Biyajima M, Mizoguchi T, Nakajima N, Suzuki N, and Wilk G 2006 *Eur. Phys. J. C* **48** 597
- [6] Lao H-L, Liu F-H and Lacey R A 2017 *Eur. Phys. J. A* **53** 44 [Erratum: 2017 *Eur. Phys. J. A* **53** 13]
- [7] Si R-F Li H-L and Liu F-H 2018 *Adv. High Energy Phys.* **2018** 7895967
- [8] B´ró G, Barnaföldi G G, Biró T S, Ürmössy K and Takács Á 2017 *Entropy* **19** 88
- [9] Hui J-Q, Jiang Z-J and Xu D-F 2018 *Adv. High Energy Phys.* **2018** 7682325
- [10] Cleymans J and Worku D 2012 *Eur. Phys. J. A* **48** 160
- [11] Cleymans J and Worku D 2012 *J. Phys. G: Nucl. Part. Phys.* **39** 02500
- [12] Wong C-Y and Wilk G 2013 *Phys. Rev. D* **87** 114007
- [13] Wong C-Y, Wilk G, Cirto L J L and Tsallis C 2015 *Phys. Rev. D* **91** 114027
- [14] Azmi M D and Cleymans J 2014 *J. Phys. G: Nucl. Part. Phys.* **41** 065001
- [15] Azmi M D and Cleymans J 2015 *Eur. Phys. J. C* **75** 430
- [16] Grigoryan S 2017 *Phys. Rev. D* **95** 056021
- [17] Acharya S et al. 2019 *Phys. Lett. B* **788** 166
- [18] Schnedermann E, Sollfrank J and Heinz U W 1993 *Phys. Rev. C* **48** 2462
- [19] Chatterjee S, Das S, Kumar L, Mishra D, Mohanty B, Sahoo R and Sharma N 2015 *Adv. High Energy Phys.* **2015** 349013
- [20] Retiere F and Lisa M A 2004 *Phys. Rev. C* **70** 044907
- [21] Prorok D 2019 *Eur. Phys. J. A* **55** 37
- [22] Motornenko A, Vovchenko V, Greiner C and Stoecker H 2019 arXiv:1908.11730 [hep-ph]
- [23] Tanabashi M et al. 2018 *Phys. Rev. D* **98** 030001
- [24] Wheaton S, Cleymans J and Hauer M 2009 *Comput. Phys. Commun.* **180** 84
- [25] Ding H-T, Karsch F, and Mukherjee S 2015 *Int. J. Mod. Phys. E* **24** 1530007
- [26] Sharma N, Cleymans J, Hippolyte B and Paradza M 2019 *Phys. Rev. C* **99** 044914
- [27] Vovchenko V, Dönigus B and Stoecker H 2019 arXiv:1906.03145 [hep-ph]
- [28] Bjorken J D 1983 *Phys. Rev. D* **27** 140